BIOCHEMISTRY
including biophysical chemistry & molecular biology

ARTICLE

pubs.acs.org/biochemistry

Unraveling Terminal C-Domain-Mediated Condensation in Fungal Biosynthesis of Imidazoindolone Metabolites

Stuart W. Haynes,[†] Brian D. Ames,[†] Xue Gao,[‡] Yi Tang,[‡] and Christopher T. Walsh*[,†]

[†]Department of Biological Chemistry and Molecular Pharmacology, Harvard Medical School, 240 Longwood Avenue, Boston, Massachusetts 02115, United States

[‡]Department of Chemical and Biomolecular Engineering and Department of Chemistry and Biochemistry, University of California Los Angeles, 420 Westwood Plaza, Los Angeles, California 90095, United States

Supporting Information

ABSTRACT: The fungal peptidyl alkaloids of the tryptoquialanine and fumiquinazoline families are nonribosomally assembled by annulation of the indole side chain of fumiquinazoline F (FQF) with an alaninyl or aminoisobutyryl unit by monomodular NRPS enzymes containing adenylation, thiolation, and condensation (A-T-C) domains. The Af12060 and Af12050 enzyme pair from *Aspergillus fumigatus* thereby converts FQF to FQA, while the homologous TqaH and TqaB enzyme pair from *Penicillium aethiopicum* makes the 2′-epi diastereomer of FQA, differing only in the stereochemistry of one of the C−N bonds formed in the annulation with L-Ala. To evaluate the basis for this stereochemical control, we have mixed and matched the flavoprotein oxygenases Af12060 and TqaH with the A-T-C modular enzymes Af12050 and TqaB to show that the NRPS enzymes control the stereochemical outcome. The terminal 50 kDa condensation domains of Af12050 and TqaB are solely responsible for the stereochemical control as shown both by making chimeric (e.g., A-T-C* and A*-T*-C) forms of these monomodular NRPS enzymes and by expression, purification, and assay of the excised C-domains. The Af12050 and TqaB condensation domains are thus a paired set of diastereospecific annulation catalysts that act on the fumiquinazoline F scaffold.

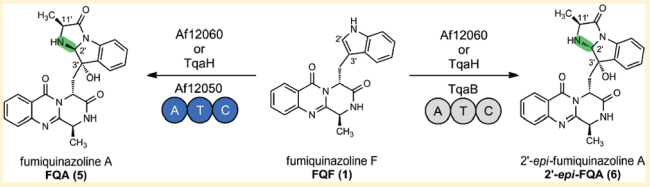

Nonribosomal peptide synthetase (NRPS) assembly lines are prevalent in the biosynthesis of secondary metabolites among a wide variety of bacterial and fungal species. Fungi have been postulated and shown to produce a variety of compounds of intriguing biological activity and structure by NRPS-based mechanisms. The peptaibols, a subgroup of peptaibiotics, have been isolated from a variety of soil-dwelling fungi and shown to exhibit antibacterial, antifungal, and anticancer properties.[1−3] Clavicipitaceae family fungi, notably *Claviceps purpurea*, produce a group of multicyclic peptides appended to a core structure of D-lysergic acid, several of which (or synthetic derivatives thereof) are in use as agents to treat a number of disorders of the vascular and central nervous systems.[4,5] A group of prenylated indole alkaloids derived from the diketopiperazine brevianamide F (*cyclo*-L-Trp-L-Pro), including the tryptostatins, which are detected in *Aspergillus fumigatus* extracts, have been used as promising candidates for the development of anticancer drugs.[6,7] Members of the tryptostatin family are also known tremorgenic mycotoxins, which act on the central nervous system of vertebrate animals that feed on foodstuffs contaminated with tremorgen-producing molds and can result in tremors, seizures, and convulsions.[8,9] Another tremorgenic mycotoxin, tryptoquialanine from *Penicillium aethiopicum*, has recently been shown to be produced by a fungal NRPS-based system.[10] Insight into the biosynthesis of tryptoquialanine revealed pathway intermediates that are remarkably similar to the fumiquinazolines, a group of cytotoxic metabolites isolated from the opportunistic human pathogen *A. fumigatus*.[11,12] These examples highlight the importance of NRPS-based mechanisms for the production of an arsenal of secondary metabolites by fungi, thus making their study of potentially vast intellectual and medicinal value.

NRPSs are often found as multimodular megasynthases, where a single massive protein comprised of multiple catalytic domains is involved in the biosynthesis of large peptidyl scaffolds. Minimally, a single NRPS module consists of adenylation (A), carrier protein/thiolation (T), and condensation (C) domains. A-Domain-catalyzed activation of an amino acid unit as the corresponding acyl-AMP mediates the attachment to the 4′-phosphopantetheine (ppt) prosthetic arm of the T-domain, forming an acyl−thioester intermediate. The T-domain-tethered acyl thioester is then delivered to the active site of a C-domain, which catalyzes amide bond formation.[13−15] In bacterial NRPSs, the completed peptide is normally transferred to an active site serine of a terminal thioesterase (TE) domain, which mediates chain release by hydrolysis or macrocyclization. A noticeably distinct feature of most fungal NRPSs is the replacement of the

Received: April 1, 2011
Revised: May 17, 2011
Published: May 17, 2011

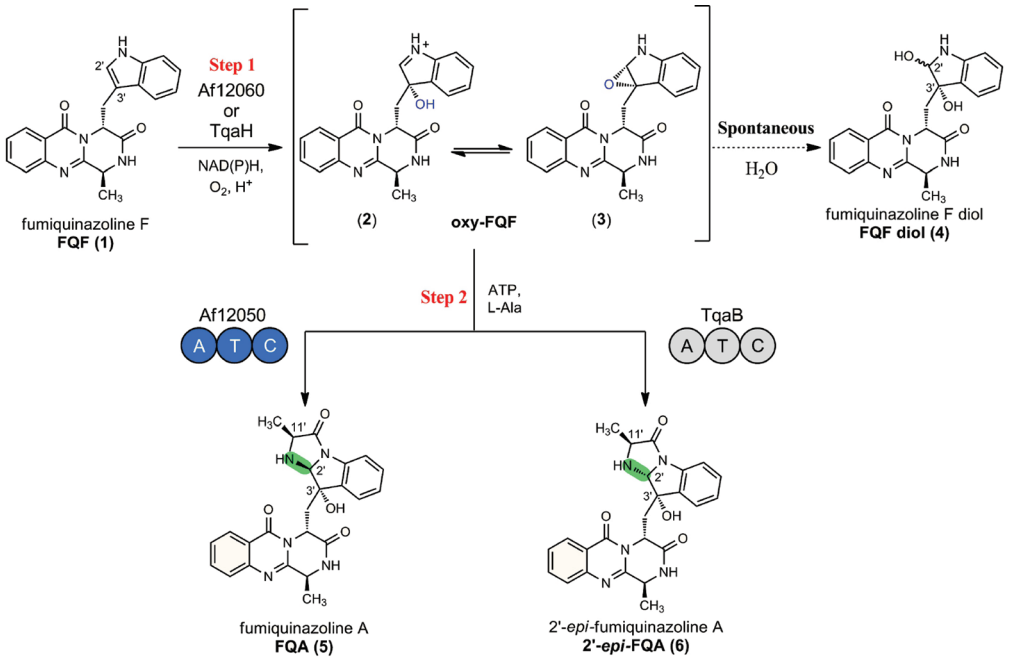

Figure 1. Stereochemical divergence of biosynthetic intermediates mediated by the action of a monomodular NRPS, Af12050 or TqaB, and illustration of spontaneous formation of the diol shunt metabolite from oxidized intermediate **2** or **3**.

TE domain with a terminal condensation, reductive, or thiolation domain.[16,17]

Such terminal C-domains of fungal NRPSs may catalyze the chain release of the peptide via cyclization by mediating the attack of intramolecular or intermolecular nucleophiles. Terminal C-domain-mediated cyclizations have been proposed to be key termination steps in the biosynthesis of several fungal NRPS products. The terminal C-domain of the bimodular NRPS (ftmA), which has been shown to be sufficient for the heterologous production of the tryprostatin precursor brevianamide F, appears likely to control the concomitant cyclization and cleavage of the *cyclo*-L-Trp-L-Pro product.[18] Terminal C-domains of fungal NRPSs have also been postulated to control the macrocyclization of large rings during the biosynthesis of cyclosporine in *Tolypocladium niveum*[19,20] and ferricrocin, a siderophore essential for *Aspergillus nidulans* viability.[21] Furthermore, the carboxy-terminal C-domain of the trimodular NRPS TqaA is postulated to be required for the production of fumiquinazoline F, the tricyclic imidazoindolone precursor of tryptoquialanine.[22] However, although terminal C-domains are cited as controlling the cyclization of NRPS-based intermediates, there is as yet no experimental evidence to illustrate their proposed catalytic activity.

We have recently reported that a monomodular NRPS (of domain structure A-T-C) from the fumiquinazoline pathway in *A. fumigatus* catalyzes the formation of fumiquinazoline A (FQA) from an activated oxidation product of fumiquinazoline F (FQF).[23] Comparison of FQA biosynthesis to the recently described tryptoquialanine (TQA) pathway of *P. aethiopicum* reveals closely related enzymatic logic for the generation of early pathway intermediates.[10] Both pathways are proposed to use a trimodular NRPS to condense and cyclize anthranilate (Ant), Trp, and Ala to form FQF, and an FAD-dependent monooxygenase and monomodular NRPS for the oxidative acylation of FQF to form a tricyclic imidazoindolone framework. In FQA biosynthesis, oxidation across C2′ and C3′ of the pendant indole of FQF by the monooxygenase Af12060 is followed by alkylation with a unit derived from L-alanine catalyzed by the monomodular NRPS Af12050. In TQA biosynthesis, the monooxygenase TqaH [56 and 76% identical and similar, respectively, to Af12060 (Figure S1 of the Supporting Information)] and monomodular NRPS TqaB [53 and 75% identical and similar, respectively, to Af12050 (Figure S2 of the Supporting Information)] are postulated to catalyze an analogous process but yield a product with the opposite stereochemistry at C2′ and a *gem*-dimethyl at C11′ (the dimethyl group results from the preferential coupling of 2-AIB by TqaB). A small amount of the C2′ epimer of FQA (2′-*epi*-FQA) has also been observed in *P. aethiopicum* extracts, arising from TqaB-mediated coupling of L-Ala[10] (Figure 1).

The basis for the difference in stereochemistry at C2′ is likely to be dictated by FQF oxidation (by Af12060 or TqaH) or amino acid coupling (by Af12050 or TqaB). Because the stereochemistry of the C3′ hydroxyl group of FQA is identical to that found in 2′-*epi*-FQA, we hypothesize that Af12060 and TqaH catalyze the same stereospecific C3′ hydroxylation of FQF. Consequently, we believe that the monomodular NRPS Af12050 or TqaB, and specifically the carboxy-terminal C-domain, directs a specific stereochemical outcome at C2′ during amino acid coupling to the oxidized FQF scaffold (Figure 1). Although the consequences of the structural differences between FQA and 11′-dimethyl-2′-*epi*-FQA with regard to biological activity and the effect on downstream enzymatic events are currently unknown, this differentiation provides an interesting example of divergence of secondary metabolite populations and divergent evolution of the corresponding biosynthetic enzymes.

The similarities between FQA from *A. fumigatus* and 2′-*epi*-FQA from *P. aethiopicum*, in terms of both structure and anticipated biosynthetic routes, provide an opportunity to study the role of the terminal C-domain of the monomodular NRPSs in

dx.doi.org/10.1021/bi2004922 |*Biochemistry* 2011, 50, 5668–5679

catalyzing regio- and stereospecific nucleophilic addition. In this work, we reconstitute the activity of both the intact proteins and excised C-domains from Af12050 and TqaB of the fumiquinazoline and tryptoquialanine pathways, respectively, to explore the function of the terminal C-domains in the enantioselective annulation of amino acids to indole in fungal alkaloid biosythesis. Our biochemical and bioinformatic analysis presents the first clear evidence of the catalytic activity and biological context of C-terminal condensation domains of fungal monomodular NRPSs.

EXPERIMENTAL PROCEDURES

General Materials and Methods. *N*-Acetylcysteamine, diisopropylethylamine, anhydrous DCM, potassium carbonate, sodium bicarbonate, potassium hydrogen sulfate, coenzyme A trilithium salt, THF, and L-[U-^{14}C]Ala (128 mCi/mmol) were all purchased from Sigma-Aldrich and used as supplied. PyBOP was purchased from ChemPep Inc. N-BOC-L-Ala-OH and pET expression vectors were purchased from EMD Chemicals. Oligonucleotide primers were purchased from Integrated DNA Technologies (Coralville, IA). Polymerase chain reactions (PCRs) were conducted using Phusion High-Fidelity PCR MasterMix (New England Biolabs). Plasmid DNA was propagated in *Escherichia coli* XL1 Blue (Stratagene) and prepared using the QIAprep Spin Mini Kit (Qiagen). DNA sequencing to confirm the correct construction of expression vectors was performed by Genewiz (South Plainfield, NJ). Protein concentrations were determined spectrophotometrically using theoretical extinction coefficients obtained from the online ProtParam tool.[24] An Agilent Technologies 6520 Accurate-Mass QTOF instrument was used for high-resolution LC−MS analysis and a Beckman Coulter Gold instrument equipped with diode array detection for reverse phase HPLC. Liquid scintillation counting was performed with a Beckman Coulter LS 6500 instrument. NMR data were collected on Varian 600 and 400 MHz spectrometers using the residual solvent peak from incomplete deuteration as an internal standard ($CDCl_3$, δ 7.26; D_2O, δ 4.75; MeCN, δ 1.94).

Synthesis of L-Ala Coenzyme A Thioester. Potassium carbonate (14 mg, 0.102 mmol, 4.0 equiv) was added to a stirred solution of N-BOC-L-Ala (5 mg, 0.026 mmol, 1.0 equiv) and PyBOP (27 mg, 0.051 mmol, 2.0 equiv) in THF and H_2O (50:50, 2 mL) at room temperature. To the resulting clear and colorless solution was added coenzyme A trilithium salt (20 mg, 0.026 mmol, 1.0 equiv), and the reaction mixture was stirred until completion as judged by LC−MS analysis (~2 h). THF was then removed in vacuo, and an equal volume of TFA (~1 mL) was added to the aqueous residue at 0 °C. The mixture was then stirred until deprotection was complete (~1 h) to give the named product in 58% yield over two steps. Solvent was then removed in vacuo and the residue purified by preparative HPLC on a Beckmann Coulter Gold system equipped with a reverse phase C18 column (Phenomenex Luna, 250 mm × 21.2 mm, 10 μm) with detection at 234 nm. Solvent system A (water with 0.1% TFA) and B (acetonitrile with 0.1% TFA) was held at 1% B for 1 min and then run over a linear gradient from 1 to 20% B over 20 min, followed by a gradient from 20 to 95% B over 2 min, before being held at 95% B for 7 min; the column was then equilibrated back to initial conditions by returning to 1% B and holding for 6 min. The peak with a retention time of 15 min was collected: ^{1}H NMR (D_2O, 600 MHz) δ 0.82 (s, 3H), 0.93 (s, 3H), 1.58 (d, J = 6.46 Hz, 3H), 2.45 (m, 2H), 3.15 (m, 2H), 3.40 (m, 2H), 3.45 (m, 2H), 3.60 (dd, J = 9.39, 4.11 Hz, 1H), 3.83 (dd, J = 9.39, 4.11 Hz, 1H), 4.03 (s, 1H), 4.26 (m, 2H), 4.35 (q, J = 6.46 Hz, 1H), 4.59 (m, 1H), 4.86 (m, 2H), 6.21 (m, 1H), 8.43 (s, 1H), 8.67 (s, 1H); HRMS m/z calcd for $C_{24}H_{41}N_8O_{17}P_3S$ 861.1415 $[M + Na]^+$, found 861.1417.

Synthesis of L-Ala SNAC. Diisopropylethylamine (0.74 mL, 4.24 mmol, 4.0 equiv) was added to a stirred solution of N-BOC-L-Ala (0.20 g, 1.06 mmol, 1.0 equiv) and PyBOP (1.10 g, 2.12 mmol, 2.0 equiv) in DCM (5 mL) at room temperature. To the resulting clear and colorless solution was added *N*-acetylcysteamine (0.12 mL, 1.16 mmol, 1.1 equiv), and the reaction was monitored by TLC and the mixture stirred until the reaction was complete (~1 h). The solvent was then removed in vacuo and the residue dissolved in ethyl acetate (25 mL). The organic layer was then washed successively with 5% $KHSO_4$ (3 × 10 mL), 5% $NaHCO_3$ (3 × 10 mL), and brine (10 mL). The extract was then dried over magnesium sulfate and evaporated to dryness in vacuo to leave a residue of colorless oil and white solid that was purified by flash column chromatography on silica gel (50−100% ethyl acetate/hexane mixture) to give N-BOC-L-Ala SNAC as a hygroscopic white solid (Figure S9A of the Supporting Information). N-BOC-L-Ala SNAC was dissolved in DCM (1 mL) and cooled to 0 °C, and TFA (1 mL) was added dropwise. The resulting mixture was stirred at 0 °C for 1 h. Solvent was then removed in vacuo, and the resulting residue was washed sequentially with DCM, diethyl ether, and an ethyl acetate/hexane mixture (1:1) to give L-Ala SNAC as a colorless sticky oil in 65% yield over two steps. A small portion of this material was further purified by preparative HPLC on a Beckmann Coulter Gold system equipped with a reverse phase C18 column (Phenomenex Luna, 250 mm × 21.2 mm, 10 μm) with detection at 234 nm. Solvent system A (water with 0.1% TFA) and B (acetonitrile with 0.1% TFA) was held at 1% B for 1 min and then run over a linear gradient from 1 to 20% B over 20 min, followed by a gradient from 20 to 95% B over 2 min, before being held at 95% B for 7 min; the column was then equilibrated back to initial conditions by returning to 1% B and holding for 6 min. The peak with a retention time of 13 min was collected: ^{1}H NMR (D_2O, 400 MHz) δ 1.58 (d, J = 7.43 Hz, 3H), 1.94 (s, 3H), 3.11 (m, 1H), 3.21 (m, 1H), 3.40 (td, J = 6.26, 2.74 Hz, 2H), 4.36 (m, 1H); HRMS m/z calcd for $C_7H_{14}N_2O_2S$ 191.0849 $[M + H]^+$, found 191.0853.

Cloning of TqaH, Stand-Alone C- and T-Domains, and Chimeric Constructs. *TqaH* cDNA was amplified from *P. aethiopicum* gDNA using reverse transcription PCR (RT-PCR) and cloned into the NdeI and EcoRI restriction sites of the pET28a vector for protein expression with an N-terminal His_6 tag [483 residues (53.2 kDa)].

Stand-alone C- and T-domain constructs were cloned from plasmid DNA (encoding Af12050[23] and TqaB[10]) into pET30 Xa-LIC and pET46 Ek-LIC vectors, respectively. Domain boundaries were determined by homology detection and structure prediction using the online server HHpred,[25] and primers (Table S1 of the Supporting Information) were designed to PCR amplify a nucleotide region corresponding to the following amino acids: 684−end, Af12050 C-domain [464 residues (53.4 kDa), N-terminal His_6-S tag]; 673−end, TqaB C-domain [483 residues (53.4 kDa), N-terminal His_6-S tag]; 591−678, Af12050 T-domain [103 residues (11.2 kDa), N-terminal His_6 tag]; and 581−668, TqaB T-domain [103 residues (11.2 kDa), N-terminal His_6 tag]. The boundaries for the stand-alone T- and C-domain constructs are annotated on the sequence alignment of Af12050 and TqaB (Figure S2 of the Supporting Information)

The domain boundaries determined above for the C-domains of Af12050 and TqaB were used for the generation of chimeric constructs by splice overlap extension PCR (see Table S1 of the Supporting Information for primers). Chimera **1** consists of the A- and T-domains of Af12050 (amino acids 1−683) and the C-domain of TqaB (amino acids 673−end), while chimera **2** consists of the A- and T-domains of TqaB (amino acids 1−672) and the C-domain of Af12050 (amino acids 684−end) (Figure 3A). The chimeric constructs were cloned into pET52b 3C-LIC to generate proteins containing an N-terminal Strep-tag II and a C-terminal His_6 tag [chimera **1**, 1161 residues (127.9 kDa); chimera **2**, 1159 residues (128.8 kDa)].

Protein Overproduction and Purification. Expression constructs for Af12050, TqaB, and Af12060 have been described previously.[10,23] Af12060, TqaH, C-domains, and T-domains were overproduced in *E. coli* BL21-Gold(DE3) cells (Stratagene), while Af12050, TqaB, and the chimeras were overproduced in *E. coli* BAP1[26] for the production of phosphopantetheinylated (holo) proteins. The production and purification of proteins were performed in a similar manner. Two to four liters of cells were grown at 37 °C in LB with the appropriate antibiotic (50 μg/mL kanamycin or 100 μg/mL carbenicillin) to an OD_{600} between 0.4 and 0.8, and the temperature was lowered to 16 °C prior to induction with 0.2 mM IPTG. Cells were harvested 18−24 h postinduction by centrifugation, suspended in lysis buffer [25 mM Tris-HCl (pH 7.5), 300 mM NaCl, 20% glycerol, 0.1% Tween 20, and 1× protease inhibitor cocktail (SigmaFast, EDTA-free)], and lysed using an EmulsiFlex-C5 homogenizer (Avestin). Insoluble material was removed by centrifugation (35000*g*) and soluble protein applied to 1−2 mL of Ni-NTA (Qiagen). Ni affinity purification was performed by batch binding protein for 30 min at 4 °C; Ni resin was washed with 2 × 25 mL of buffer A [50 mM Tris-HCl (pH 7.5), 300 mM NaCl, 10% glycerol, and 0.1 mM EDTA] containing 20 mM imidazole and protein eluted with buffer A containing 250 mM imidazole (2 × 5 mL). The elutions were pooled and concentrated using centrifugal filtration devices (Amicon), flash-frozen in liquid N_2, and stored at −80 °C (except for TqaB, which was kept at 4 °C because of its instability during freezing and thawing).

Assay for Phosphopantetheinylation of the Af12050 and TqaB T-Domain Constructs with [1-^{14}C]Acetyl-CoA. Reaction mixtures (50 μL) contained 25 μM [1-^{14}C]acetyl-CoA (0.075 μCi), 250 nM *Bacillus subtilis* Sfp,[27] and 10 μM T-domain in buffer [50 mM sodium phosphate (pH 7.5), 5 mM $MgCl_2$, 100 mM NaCl, 1 mM TCEP, and 5% glycerol]. Reactions were initiated by addition of Sfp and mixtures incubated at 25 °C for 1, 2.5, 5, or 10 min prior to reactions being quenched with 0.5 mL of 10% TCA (containing 50 μg of BSA). Protein precipitate was pelleted by centrifugation, washed twice with 10% TCA, and dissolved in 80% formic acid for liquid scintillation counting (Figure S3 of the Supporting Information).

Single-Time Point HPLC-Based Assays for Monooxygenase and NRPS Activity. Reaction mixtures contained the required components as listed below. Reactions were initiated by the addition of monooxygenase (Af12060 or TqaH) and mixtures incubated at room temperature overnight (14−16 h). Reactions were then quenched by the addition of an equal volume of acetonitrile; the precipitant was removed by centrifugation, and 20 μL samples of the resulting supernatant were injected for HPLC analysis on a Beckmann Coulter Gold system equipped with an Alltima C18 reverse phase column (150 mm × 4.6 mm, 5 μm). Solvent system A (water with 0.1% TFA) and B (acetonitrile with 0.1% TFA) was held at 25% B for 1 min and then run over a linear gradient from 25 to 55% B over 20 min, followed by a gradient from 55 to 95% B over 1 min, before being held at 95% B for 2.5 min; the column was then equilibrated back to initial conditions by returning to 25% B and holding for 5 min.

Monooxygenase Activity Assays (Af12060 and TqaH). Reaction mixtures (100 μL) contained 2.5 μM Af12060 or TqaH, 2 mM NADH, and 250 μM FQF in NaP_i buffer [50 mM sodium phosphate (pH 7.5), 100 mM NaCl, and 5% glycerol]. The reaction mixture containing Af12060 was scaled up to 15 mL to allow for isolation and characterization of FQF diol; the same reaction components and concentrations used on the small scale were used here with the exception of FQF, which was used at a concentration of 500 μM. FQF diol was purified from the resulting mixture by the following procedure. Enzyme was removed from the incubation by centrifugal filtration (30 kDa molecular mass cutoff). The filtrate was then purified by preparative HPLC on a Beckmann Coulter Gold system equipped with a reverse phase C18 column (Phenomenex Luna, 250 mm × 21.2 mm, 10 μm) with detection at 230 nm. Solvent system A (no additive) and B (no additive) was held at 30% B for 1 min and then run over a linear gradient from 30 to 60% B over 20 min, followed by a gradient from 60 to 95% B over 2 min, before being held at 95% B for 7 min; the column was then equilibrated back to initial conditions by returning to 30% B and holding for 5 min. The peak with a retention time of 14.5 min was collected. This peak was shown to consist of a mixture of diol and multiple dimerization products and further purified by solid phase extraction over a Sep-Pak C18 cartridge (Waters) according to the following protocol using D_2O and d_6-acetonitrile. The column was wet with 10 column volumes (CV) of d_6-acetonitrile (∼6 mL) and then flushed with 10 CV of D_2O. The sample was loaded on the column in 500 μL of D_2O and washed with 4 CV of D_2O (2.4 mL). Bound products were then eluted from the column and collected as 600 μL fractions using a 30% d_6-acetonitrile/D_2O mixture (4 × 600 μL), a 50% d_6-acetonitrile/D_2O mixture (4 × 600 μL), and a 90% d_6-acetonitrile/D_2O mixture (4 × 600 μL). HPLC analysis of the resulting fractions was used to determine the presence of pure FQF diol, and the sample was analyzed directly by NMR spectroscopy.

For FQF diol spectroscopic characterization and assignments, see Table S2 of the Supporting Information: HRMS *m*/*z* calcd for $C_{21}H_{20}N_4O_4$ 375.1452 $[M - H_2O + H]^+$, found 375.1458.

*Monomodular NRPS Activity Assays (Af12050, TqaB, chimera **1**, and chimera **2**).* Reaction mixtures (100 μL) contained 2.5 μM Af12060, 5 μM holo-NRPS, 1 mM ATP, 2 mM $MgCl_2$, 1 mM L-Ala, 2 mM NADH, and 250 μM FQF in NaP_i buffer. The reaction mixture containing TqaB was scaled up to 30 mL to allow for isolation and characterization of 2′-*epi*-FQA; the same reaction components and concentrations used on the small scale were used here with the exception of FQF, which was used at a concentration of 500 μM. 2′-*epi*-FQA was purified from the resulting mixture by the following procedure. An equal volume of acetonitrile was added to the incubation, and the precipitated protein was pelleted by centrifugation. The supernatant was then decanted, the acetonitrile removed in vacuo, and the residual water removed by lyophilization. The resulting residue was taken up in 25% acetonitrile and water and purified by preparative HPLC on a Beckmann Coulter Gold system equipped with a reverse phase C18 column (Phenomenex Luna, 250 mm × 21.2 mm, 10 μm) with detection at 254 nm. Solvent system A (water with 0.1% TFA) and B (acetonitrile with 0.1% TFA) was

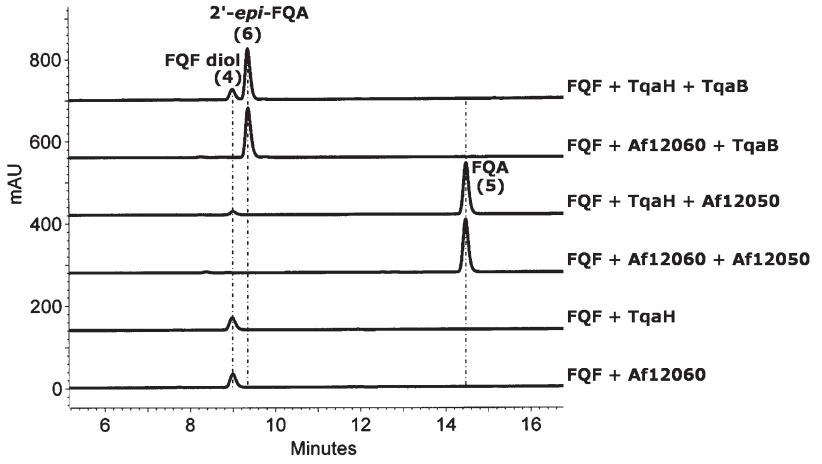

Figure 2. HPLC analysis at 254 nm of reaction mixtures containing 2.5 μM monooxygenase (Af12060 or TqaH), 2 mM NADH, and 250 μM FQF in NaP_i buffer, in addition to 5 μM holo-NRPS (Af12050 or TqaB), 1 mM ATP, 2 mM $MgCl_2$, and 1 mM L-Ala when both monooxygenase and monomodular NRPS are included.

held at 25% B for 1 min and then run over a linear gradient from 25 to 53% B over 30 min, followed by a gradient from 53 to 95% B over 1 min, before being held at 95% B for 5 min; the column was then equilibrated back to initial conditions by returning to 25% B and holding for 8 min. The peak with a retention time of 25 min was collected.

For 2′-*epi*-FQA spectroscopic characterization and assignments, see Table S3 of the Supporting Information: HRMS *m*/*z* calcd for $C_{24}H_{23}N_5O_4$ 446.1823 $[M + H]^+$, found 446.1824.

Stand-Alone C-Domain Activity Assays (Af12050 and TqaB). The ability of the C-domain constructs to catalyze coupling of alanine to oxy-FQF was tested using L-Ala SNAC as a free-standing substrate, and also using a tethered L-alanyl-S-T-domain intermediate as a substrate (prepared via coupling of L-Ala-CoA to the holo-Af12050 T-domain). Reaction mixtures with L-Ala SNAC as a substrate contained 1 μM Af12060, 10 μM C-domain, 1 mM L-Ala SNAC, 2 mM NADH, and 250 μM FQF in NaP_i buffer. Reaction mixtures for the assay with L-alanyl-S-T-domain as a substrate contained 1 μM Af12060, 10 μM C-domain, 50 μM Af12050 T-domain, 1 μM Sfp,[27] 1 mM L-Ala-CoA, 2 mM $MgCl_2$, 2 mM NADH, and 250 μM FQF in NaP_i buffer. Prior to initiation of the reaction with monooxygenase, the reaction mixture containing L-Ala-CoA was incubated for 10 min to allow for the Sfp-catalyzed loading of alanine onto the T-domain. Following incubation for 120 min at room temperature, the reactions (100 μL) were quenched with an equal volume of acetonitrile and 20 μL samples analyzed by analytical HPLC as described above.

Time Course HPLC-Based Assays for 2′-*epi*-FQA Formation. A 250 μL initial reaction mixture was set up, and 50 μL aliquots were quenched with an equal volume of acetonitrile 15, 30, 60, and 120 min after the addition of Af12060. To follow the nonenzymatic rate of 2′-*epi*-FQA formation, we combined 1 μM Af12060, 2 mM NADH, 250 μM FQF, and 1 mM L-Ala or 1 mM L-Ala SNAC or 1 mM L-Ala-CoA in NaP_i buffer. The enzymatic rate of 2′-*epi*-FQA formation was determined by the addition of 10 μM TqaB C-domain. For full-length TqaB, we combined 2.5 μM Af12060, 10 μM holo-TqaB, 1 mM ATP, 2 mM $MgCl_2$, 1 mM L-Ala, 2 mM NADH, and 250 μM FQF in NaP_i buffer. Quenched and clarified samples were assessed via analytical HPLC as described above. For each time point, the peak corresponding to 2′-*epi*-FQA was integrated and converted to a concentration using a standard curve made by injecting 20 μL samples at a known concentration (determined using an extinction coefficient calculated for 2′-*epi*-FQA at 256 nm of 10532 M^{-1} cm^{-1}). Plotting the concentration of 2′-*epi*-FQA versus time allowed for the calculation of initial rate data (Figure S4 of the Supporting Information).

RESULTS

Examination of the Effect of Monomodular NRPS and Monooxygenase. To gain initial insight into the enzymatic requirements for directing the stereochemical course of dual N−C bond formation for coupling of alanine to oxy-FQF, we mixed and matched combinations of NPRS (Af12050 and TqaB) and monooxygenase (Af12060 and TqaH) and analyzed their respective products. The production and characterization of Af12050 and Af12060 have been previously described;[23] for comparative analysis, we overproduced TqaH and TqaB as the corresponding His_6-tagged proteins from *E. coli* and purified them via Ni-NTA affinity chromatography. Interestingly, though TqaH and Af12060 are 76% similar at the amino acid level, their expression profiles, purities, and flavin contents vary significantly (Figures S1 and S5 of the Supporting Information). Incubation of FQF with TqaH generated a peak with a retention time of 9 min that is identical to that seen upon incubation of FQF with Af12060 (Figure 2). Isolation and characterization of this compound were hindered by rapid decomposition to a complex mixture of apparent dimerization products upon concentration and lyopholization (post-preparative HPLC). However, removal of the dimerization products by SPE (Sep-Pak C18) allowed us to identify this product by one- and two-dimensional NMR experiments as a diol shunt product [FQF diol (Figure 1)]. The FQF diol arises from the quenching of the predicted unstable oxy-FQF epoxide/hydroxy imine product of Af12060 (or TqaH) with water. Co-incubation of TqaH with the monomodular NRPS from *A. fumigatus*, Af12050, resulted in the production of a compound matching the retention time and UV pattern (Figure S6 of the Supporting Information) of FQA as previously characterized from an in vitro reconstitution of the natural Af12060/Af12050 system (Figure 2). By comparison when the

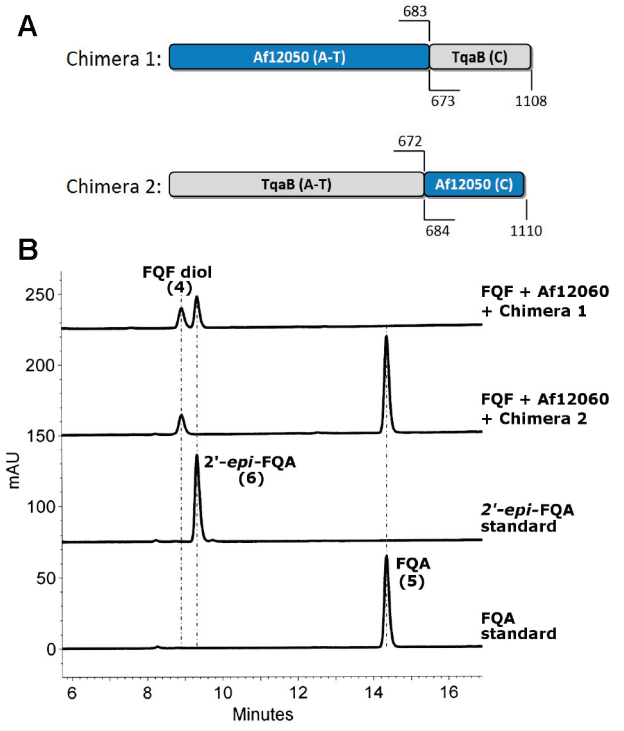

Figure 3. (A) Cartoon representation of the structure of chimeras **1** and **2**. Numbers indicate the amino acid numbers from the native protein included in each chimera. (B) HPLC assay indicating the chimera-mediated formation of FQA or 2′-*epi*-FQA with detection at 254 nm.

monomodular NRPS TqaB is co-incubated with either monooxygenase (Af12060 or TqaH), a new peak is produced with a retention time of 9.4 min (Figure 2). This compound was isolated in sufficient quantity for investigation by NMR spectroscopy and structurally characterized as the C2′ epimer of FQA (2′-*epi*-FQA). These experiments clearly illustrate that it is the activity of the monomodular NRPS that determines the stereochemical outcome of this reaction and not that of the monooxygenase.

Construction of C-Domain-Swapped Chimeric Proteins. With the knowledge that the monomodular NRPSs Af12050 and TqaB (and not the monooxygenases) direct the stereochemical outcome at C2′ of FQA and *epi*-FQA, respectively, we then wanted to test the hypothesis that the divergent NRPS-based activities could be specifically attributed to the carboxy-terminal C-domains of Af12050 and TqaB. To investigate this hypothesis, we constructed two hybrid (or chimeric) proteins. The C-domains of TqaB and Af12050 were swapped, resulting in one protein containing the A- and T-domains from Af12050 and the C-domain from TqaB (chimera **1**) and another protein with the A- and T-domains from TqaB and the C-domain from Af12050 (chimera **2**) (Figure 3A). For the purposes of cloning, the linker region between the T- and C-domains was defined by a combination of sequence alignment and secondary and tertiary structure prediction using HHpred.[25] In particular, modeling of tertiary structure using the bidomain TycC T_5-C_6 structure as a template (Protein Data Bank entry 2jgp[28]) indicated an unstructured linker of 30 residues for both Af12050 (amino acids 669−698, TASV...RKSQ) and TqaB (amino acids 659−687, VKQP...AKCQ). To allow for flexibility with regard to the predicted versus actual structure of the corresponding T- and C-domains, we chose a C-domain swap point of Q684 of Af12050 and Q673 of TqaB, which lies near the middle of the predicted unstructured linker region. Hybrid constructs were then generated using splice overlap extension PCR.

The enzymatic activity of chimera **1** was demonstrated in vitro by incubation with FQF, monooxygenase (Af12060), and the required cofactors and shown to produce two peaks, one peak with a retention time, HRMS, and characteristic UV pattern matching that of the FQF diol and the other matching that of 2′-*epi*-FQA. Incubation of chimera **2** produced two peaks, one corresponding to FQF diol and the other matching the retention time and UV pattern of FQA (Figure 3). The ability of the chimeric constructs to activate and load a variety of amino acids was investigated by reconstituting their activity in vitro in the presence of L-Ala, D-Ala, or 2-aminoisobutyric acid (2-AIB). Chimera **1** efficiently activates, loads, and condenses L-Ala with the FQF-derived oxidized species to give 2′-*epi*-FQA. 11′-*epi*-2′-*epi*-FQA is also produced by chimera **1** when using D-Ala but at a level much lower than that seen for 2′-*epi*-FQA. A very small amount of a compound with a mass and UV pattern consistent with 11′-dimethyl-2′-*epi*-FQA is produced by chimera **1** when using 2-aminoisobutyric acid in place of alanine (Figure S7 of the Supporting Information). Similar substrate specificity investigations with chimera 2 show the efficient activation, loading, and condensation of L-Ala, D-Ala, and 2-aminoisobutyric acid to give FQA, 11′-*epi*-FQA, and 11′-dimethyl-FQA, respectively, all in substantial quantities (Figure S8 of the Supporting Information). The activities of the chimeric constructs demonstrate that it is the C-terminal C-domain of the monomodular NRPSs (Af12050 and TqaB) that account for and control their observed stereochemical control.

Demonstration of Activity of Stand-Alone C-Domains from Af12050 and TqaB. To specifically probe the catalytic activity of the respective C-domains from Af12050 and TqaB, we overexpressed the C-domain regions of TqaB and Af12050 as stand-alone His_6-tagged proteins from *E. coli* (Af12050 C-domain, 53.4 kDa, residues 684−end; TqaB C-domain, 53.4 kDa, residues 673−end). Concurrently, we cloned and expressed the T-domains from both TqaB and Af12050. The structure prediction described above for the generation of the chimeric constructs was used as the basis for cloning these stand-alone proteins. The ability of the excised T-domains to be phosphopantetheinylated was tested by incubating the apoprotein with Sfp (a promiscuous phosphopantetheinyl transferase) and [^{14}C]acetyl-CoA. Interestingly, although both proteins were expressed from *E. coli* in soluble form, only the T-domain from Af12050 was observed to be labeled by [^{14}C]acetyl-CoA [26% after 10 min compared to 1.3% for the TqaB T-domain (Figure S3 of the Supporting Information)]. MALDI-MS analysis of the TqaB T-domain revealed a mixture of both apo and holo forms in an approximately 2:1 ratio. Therefore, it is not clear why the apo TqaB T-domain present did not react with acetyl-CoA in vitro. With these protein constructs in hand, we synthesized an L-Ala coenzyme A thioester (L-Ala-CoA) via standard peptide coupling procedures and generated an L-alanyl-S-T-domain substrate by incubating L-Ala-CoA with the Af12050 T-domain and Sfp. Addition of the TqaB C-domain to the L-alanyl-S-T-domain resulted in the conversion of FQF to two new peaks corresponding to FQF-diol and 2′-*epi*-FQA (as confirmed by comparison with authentic standards). Incubating the Af12050 C-domain with the L-alanyl-S-T-domain resulted in the production of three new peaks; two large magnitude peaks indicated the presence of large quantities of FQA and the FQF-diol, and one smaller peak showed the formation of some 2′-*epi*-FQA (Figure 4).

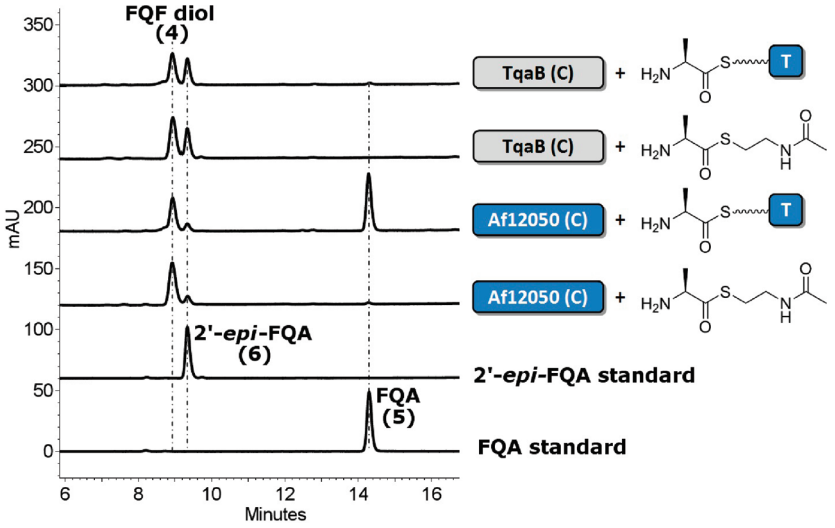

Figure 4. HPLC analysis of incubations of stand-alone C-domains from TqaB or Af12050 with L-Ala SNAC (shown as a chemical structure) and the L-alanyl-S-T-domain (shown as a T-domain-tethered cartoon).

N-Acetylcysteamine-derived L-Ala thioester (L-Ala SNAC) was also synthesized via PyBOP-mediated peptide coupling. Comparison of the products observed after the incubation of the TqaB C-domain with L-Ala SNAC and FQF with authentic standards allowed them to be confirmed as FQF-diol and 2′-*epi*-FQA, in agreement with the analogous stand-alone T- and C-domain experiment. In contrast, when the Af12050 C-domain was incubated with FQF and L-Ala SNAC, the result observed did not match that seen with the equivalent T-domain-tethered substrate as only FQF diol was produced in a significant quantity, while a small peak indicated the presence of a small amount of 2′-*epi*-FQA (Figure 4).

DISCUSSION

Fuminquinazoline A (FQA) produced by *A. fumigatus* contains an interesting pendant indole moiety derived from a tryptophan unit that has been modified by the stereospecific addition of L-alanine to form a new five-member ring resulting in a tricyclic 5−5−6 imidazoindolone framework. FQA has been shown to be the direct precursor of two further previously identified metabolites fuminquinazoline C (FQC) and fuminquinazoline D (FQD).[29] Recently, characterization of intermediates from the tryptoquialanine pathway in *P. aethiopicum* has revealed a close similarity in the early biosynthetic steps to intermediates of the FQA pathway in *A. fumigatus*. Intermediates on the pathway to tryptoquialanine that share a remarkable resemblance to FQA have been observed in mutants of *P. aethiopicum* and appear to be substrates for downstream enzymes that mediate their transformation to tryptoquialanine. Notably, 2′-*epi*-FQA identified in *P. aethiopicum* differs from FQA only in the stereochemistry at C2′ of the imidazoindolone moiety. The stereochemical difference between FQA and 2′-*epi*-FQA may influence the downstream fate of these two molecules to ultimately give FQC/FQD and tryptoquialanine, respectively. Formation of FQA from oxy-FQF in *A. fumigatus* is controlled by the action of a monomodular NRPS from the fumiquinazoline pathway (Af12050), whereas the biosynthesis of 2′-*epi*-FQA in *P. aethiopicum* has been proposed to be controlled by the action of TqaB, based on its homology to Af12050. The opposite stereochemistry at C2′ of the metabolites observed in *A. fumigatus* and *P. aethiopicum* poses the question of how the cyclization of an amino acid-derived unit that generates the observed five-member ring is controlled, specifically, how the stereochemistry of addition of the amine nucleophile to C2′ of the indole is differentially directed in FQA and 2′-*epi*-FQA biosynthesis.

Enzymatic assays of both TqaH and Af12060 revealed the product of each to be identical, whereas the activity of the A-T-C tridomain-containing Af12050 and TqaB resulted in two different products, FQA and 2′-*epi*-FQA, respectively. These data confirm the crucial role that the monomodular NRPS plays in directing the stereospecific formation of the C2′ carbon−nitrogen bond.

Determining whether the C-domain of the NRPS was in fact responsible for the facial specific addition as we proposed required the study of C-domain activity in a non-native environment. Characterization of the chimeric constructs showed that the enantiospecificity of FQA scaffold formation is consistent with that of the parent protein from which the C-domain of each chimeric construct was taken. The A-domain of Af12050 has previously been shown to preferentially activate L-Ala over D-Ala, which is in line with the observed amino acid coupling to oxy-FQF to form FQA in *A. fumigatus*.[23] On the other hand, the A-domain of TqaB exhibits much broader substrate specificity, activating not only 2-aminoisobutyric acid as observed in tryptoquialanine but also both L-Ala and D-Ala.[10] The activity of both the Af12050 and TqaB A-domains was maintained in chimera **1** and chimera **2** (Figures S7 and S8 of the Supporting Information), illustrating the persistence of A-domain substrate specificity and also the ability of the terminal C-domains to accept and couple noncognate amino acids for the generation of novel "unnatural" natural products: 11′-dimethyl-FQA and 11′-*epi*-FQA (chimera **2**) and 11′-*epi*-2′-*epi*-FQA (chimera **1**).

To the best of our knowledge, this is the first reported example of C-domain swapping yielding functional multidomain NRPS assembly lines. In previous studies, the N-terminal C-domain of the enterobactin synthetase EntF was excised and activity reconstituted in vitro,[30] adenylation domain swapping was performed,[31,32] and whole modules and domains of the tyrocidine synthetase were fused to generated hybrid enzymes.[33] In our case, we recognize that the swapped domains are the

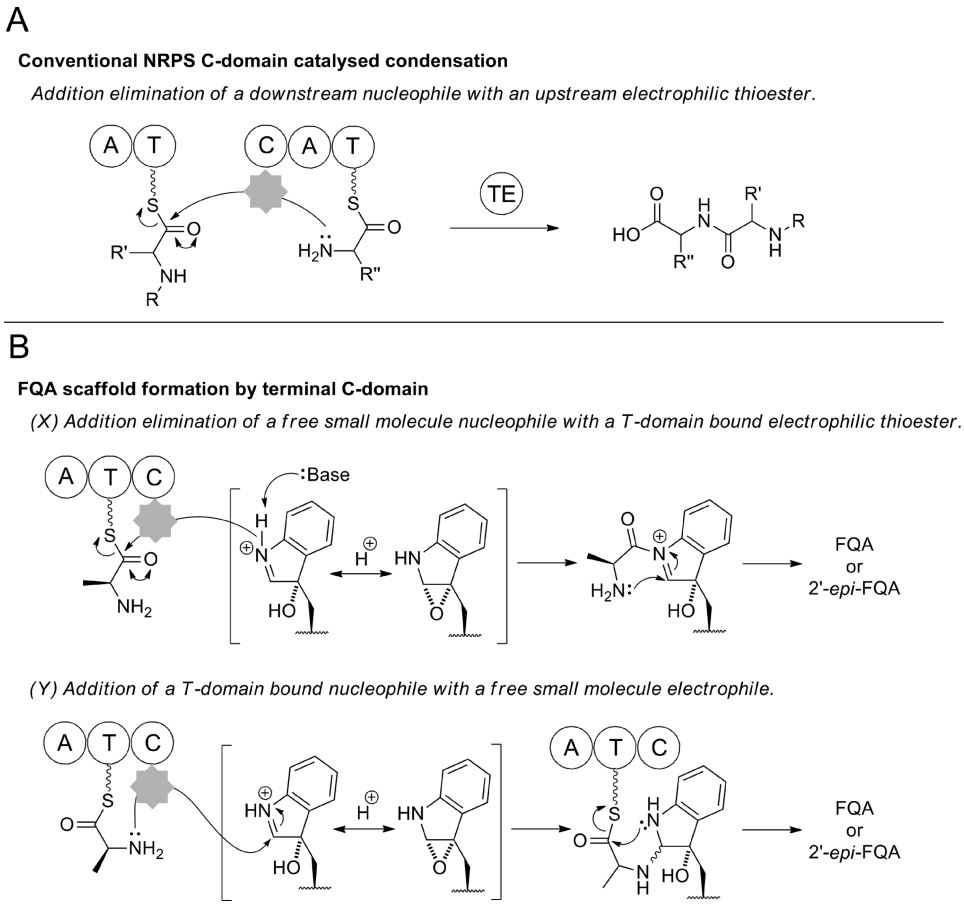

Figure 5. Schematic representation of canonical C-domain catalysis in comparison to the two proposed enzymatic routes to FQA imidazoindolone scaffold formation.

carboxy-terminal domains of monomodular proteins that are highly homologous, which facilitates the process of generating functionally intact hybrid proteins.

Expression and purification of the excised 53.4 kDa C-domains from Af12050 and TqaB in soluble form allowed us to conclusively show that the C-domain of either enzyme is all that is required for directing the stereospecific formation of an FQA (or 2′-*epi*-FQA) product. T-Domain loading with acetyl-CoA mediated by Sfp (a phosphopantetheinyl transferase from *B. subtilis*) was successful only with the T-domain of Af12050 (and not that of TqaB). The mixture of both apo and holo forms of the TqaB T-domain presumably results from the activity of an *E. coli* 4′-phosphopantetheinyl transferase (PPTase), which shows some low-level activity on the non-native T-domain. However, given that the loading of Af12050 T-domain preceeded smoothly, we did not pursue the reason for the inactivity of the TqaB T-domain further. Presumably, the inactivity of the TqaB T-domain is due to misfolding or other structurally irregularities, as perhaps is suggested by the poor *E. coli*-based overproduction of this protein. Furthermore, we reasoned that given the high degree of sequence similarity between Af12050 and TqaB T-domain regions, the T-domain used should have no bearing on the observed result. Aminoacyl-*N*-acetylcysteamine thioesters (aminoacyl-SNACs) have been shown on several occasions to act as efficient small molecule substrates of NRPS C-domains.[34] Therefore, to devise a small-molecule-based experiment complementary to the co-incubation of stand-alone T- and C-domains, we also synthesized L-Ala SNAC. The purified C-domain from TqaB was observed to specifically generate 2′-*epi*-FQA from FQF with either the L-Ala-loaded T-domain (L-alanyl-S-T-domain) or L-Ala SNAC. By contrast, the Af12050 C-domain generated FQA only when using the L-alanyl-S-T-domain as a substrate; when using the small molecule (T-domain mimic) SNAC derivative, only the shunt metabolite FQF-diol was observed in significant quantity. The appearance of a small amount of 2′-*epi*-FQA in Af12050 C-domain incubations with both the L-Ala-loaded T-domain and L-Ala SNAC provoked our interest in the mechanism of its formation. Was the Af12050 C-domain losing some degree of stereospecificity as a result of catalyzing an *in trans*-like condensation? To this end, the level of spontaneous condensation (in the absence of the TqaB C-domain) of the L-alanyl-S-T-domain and L-Ala SNAC with oxy-FQF was investigated by a time course study. These experiments revealed a background level of spontaneous 2′-*epi*-FQA formation approximately one-third the rate of C-domain-catalyzed condensation with both L-alanyl-S-T-domain and L-Ala SNAC (Figure S4 of the Supporting Information). Spontaneous (uncatalyzed) attack of the thioester substrates (L-Ala SNAC and L-alanyl-S-T-domain) by the latent nucleophilic indole NH group after dearomatization of the indole ring by epoxidation or hydroxylation appears to explain this "background" level of 2′-*epi*-FQA formation. Such an attack would be favored by the stability of the resulting amide bond, and subsequent intramolecular ring closure to give the kinetically favored five-member

dx.doi.org/10.1021/bi2004922 |*Biochemistry* 2011, 50, 5668–5679

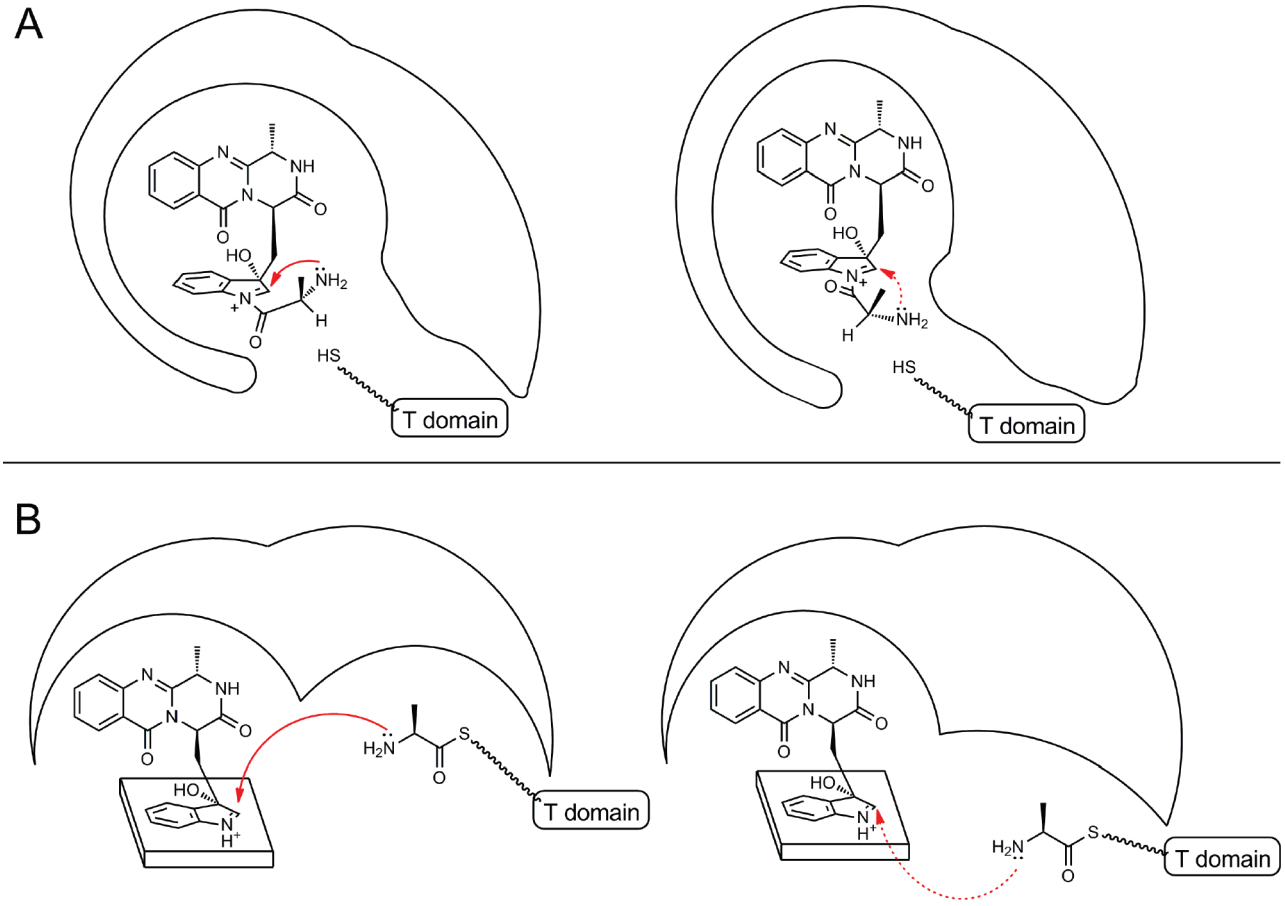

Figure 6. Cartoon illustration of proposed routes of C-domain-mediated stereospecific C−N bond formation. (A) Stereospecific formation of the C−N bond controlled by the required conformation of the amide L-Ala moiety in the C-domain active site. (B) Facial specificity of primary amine addition controlled by positioning of the incoming T-domain.

ring (to give 2′-*epi*-FQA) would be predicted to occur rapidly. Crude quantitative analysis of the levels of spontaneous formation of 2′-*epi*-FQA using UV analysis (and standard curve calibration) to quantify 2′-*epi*-FQA shows that the levels of spontaneous formation account for the observed 2′-*epi*-FQA in incubations of the Af12050 C-domain with the L-alanyl-S-T-domain and L-Ala SNAC.

The condensation of a T-domain-tethered amino acid to the oxy-FQF scaffold by the action of the terminal condensation domains of Af12050 and TqaB could proceed through two distinct pathways depending on the order of N−C bond formation. Both of these pathways differ significantly from standard C-domain chemistry (Figure 5). Classically, a C-domain would catalyze the formation of an amide bond between a T-domain-tethered upstream acyl-thioester intermediate and a nucleophile tethered to a downstream T-domain (Figure 5A).[13] The biosynthesis of FQA (or 2′-*epi*-FQA) from FQF could be envisaged to proceed via one of two routes, both of which presumably proceed by an initial C-domain-mediated addition, followed by a spontaneous intramolecular cyclization. Initial thioester cleavage by a C-domain-catalyzed addition of the indole-derived secondary amine followed by spontaneous ring closure by attack of the L-alanine-derived primary amine aligns well with the conventional function of C-domain mediation of directing nucleophilic attack on a T-domain-bound thioester (Figure 5B, pathway X). Indeed, the observation of a C-domain-catalyzing condensation with a free soluble nucleophile has been previously reported, for example, in the biosynthesis of pseudomonine where condensation of a T-domain-bound intermediate with a free amine monomer has been shown,[35] or vibriobactin biosynthesis in which a soluble small molecule derived from norspermidine acts as the incoming nucleophile.[36] Alternatively, attack of the L-alanine primary amine may precede a subsequent ring closure by intramolecular spontaneous amide bond formation (Figure 5B, pathway Y). This would require the C-domain to catalyze addition of a thioester-bound nucleophile to a free soluble electrophile, via a process currently unprecedented in the chemistry of C-domain catalysis.

Analogues of L-Ala SNAC that disfavored attack at C2′ of oxy-FQF (to form the stereospecific C−N bond) or attack at the oxidized indole NH group (to give the observed amide bond) were both synthesized (Figure S9B of the Supporting Information) in an attempt to probe the route to the dual N−C bond formation observed during the biosynthesis of the FQA imidazoindolone scaffold. Incubation of TqaB C-domain with N-acetylcysteamine thioesters derived from propionic acid or L-lactic acid, in which nucleophilic attack at C2′ of oxy-FQF is either impossible or severely hindered, both failed to yield any detectable products. L-Ala SNAC analogues in which the thioester is replaced with a thioether or amide bond to prevent or hinder amide bond formation to give FQA also failed to give any detectable products, despite the activity of the TqaB C-domain

dx.doi.org/10.1021/bi2004922 |*Biochemistry* 2011, 50, 5668–5679

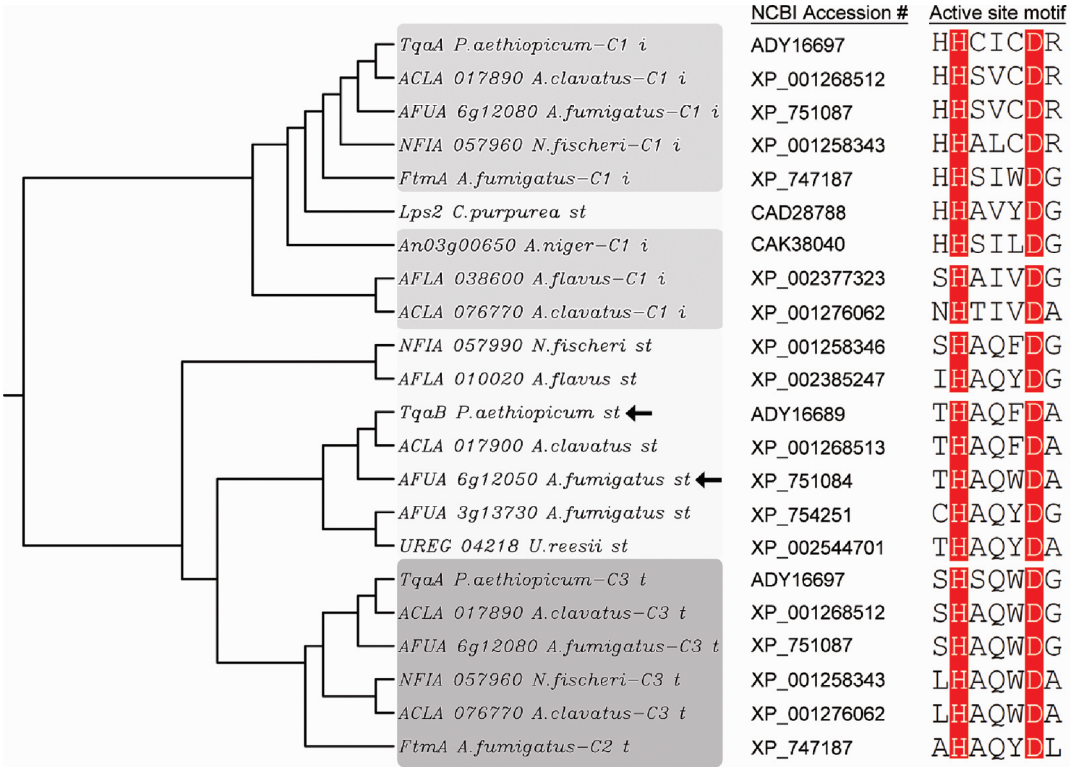

Figure 7. Neighbor-joining phylogenetic tree and active site motif of select fungal C-domains, highlighting the divergent grouping of C-domains of monomodular NRPSs (abbreviated "st" for "single-module terminal") from those internal ("i") and C-terminal ("t") of multimodular synthetases. Arrows highlight the two C-domains biochemically characterized in this work. Sequence alignment and tree construction were performed using Clustal W.[41] (For a comprehensive phylogenomic analysis of fungal NRPSs, see ref 42 and ref 17.)

with L-Ala SNAC. It is not clear why there were no products observed with either set of SNAC analogues; perhaps, the C-domain exhibits a strong specificity for L-Ala such that even close structural homologues are not accepted. At this stage, the apparent lack of a viable substrate analogue has prevented a detailed mechanistic study of this dual N−C bond formation event.

It seems that a minor configurational adjustment to the binding of the L-Ala-derived moiety or an adjustment to the position of the FQF-derived intermediate within the TqaB C-domain compared to that of Af12050 could direct the attack of the L-Ala amino group to opposite faces of the oxidized indole species (Figure 6), resulting in the observed stereochemical difference at C2′. Analysis of the C-domains of TqaB and Af12050 by homology modeling suggests the proposed FQF binding pocket (as deduced from the relative position of the acceptor binding site from the point of T-domain attachment) is remarkably similar in both enzymes. Conversely, the presumed donor binding pocket of the incoming upstream T-domain shows some significant differences in residue composition and structure. These observations led to the supposition that the binding position of FQF in both enzymes is approximately equal, and therefore, the differential binding of the L-Ala-derived moiety directs the stereospecificity of the observed reaction. To support this proposal, future investigations that shed light on C-domain structure and FQF−L-Ala binding will be essential.

If formation of FQA proceeds via pathway X (Figure 5B), then presumably the stereochemistry of the spontaneous addition of the L-alanine primary amine could be controlled by the observed enzyme conformation strictly controlling the orientation of the pendant L-alanine immediately prior to and after thioester bond cleavage (Figure 6A). If catalysis proceeds via pathway Y (Figure 5B), then control of the path of the incoming phosphantetheinyl arm to either the top or bottom face of the oxidized indole would seem to be the logical mode of stereochemical control (Figure 6B). Although intuitively it seems beneficial for the stereospecific addition to occur first such that it is catalyzed by C-domain activity, a reaction of an upstream T-domain-bound nucleophile with a free soluble electrophile has not previously been observed to be mediated by a C-domain.

The unique functionality of Af12050 and TqaB to act in concert with multimodular NRPS machinery for amino acid coupling prompted a search of sequenced fungal genomes for similar proteins (monomodular NRPSs with an A-T-C domain organization) to identify functionally similar C-domains and to improve our understanding of the occurrence and divergence of this terminal domain as part of monomodular NRPSs. While monomodular NRPSs with the A-T-R domain organization are widespread among fungal species (due in large part to the involvement of this module in fungal lysine biosynthesis[37,38]), monomodular systems ending in C-domains are much less common and are restricted almost exclusively to the Eurotiomycetes class, most notably among the genus *Aspergillus*. In addition to Af12050 and TqaB, 23 monomodular NRPSs were found with the A-T-C domain structure. Fifteen of these were identified from *Aspergillus* (or *Neosartorya*) genomes, two from *Uncinocorpus reesii*, one from *Podospora anserina*, and four in total from the Basidiomycota *Schizophyllum commune* and *Puccinia graminis*. Of the 23 found, only four are clustered next to multimodular synthetases. ACLA_017900 (part of a putative tryptoquivaline cluster) and NFIA_057990 (part of a putative fiscalin A cluster) are next to

dx.doi.org/10.1021/bi2004922 |*Biochemistry* 2011, 50, 5668–5679

trimodular NRPSs that are homologous to Af12080.[39] AFLA_010020 and AO090103000223 (orthologous genes) are found adjacent to hybrid PKS-NRPSs. In these four cases, the proximity of the mono- and multimodular NRPSs suggests a sequential action for peptide-based framework construction. For the remaining examples of A-T-C proteins, a biosynthetic role is less clear. Interestingly, in 20 of 23 cases, the catalytically important second histidine of the canonical C-domain active site motif HHxxxDG remains intact,[40] while in all cases, the structurally integral aspartic acid is conserved (Figure S10 of the Supporting Information).

A simple phylogenetic analysis of the terminal C-domains of monomodular NRPSs revealed a relatively divergent population when analyzed independently (Figure S10 of the Supporting Information); however, this population generally grouped separate from the internal and terminal C-domains of multimodular NRPSs (Figure 7). As anticipated, the terminal C-domains of monomodular NRPSs are more closely related to terminal C-domains of multimodular systems than to internal C-domains. Overall, our sequence-based search and analysis reveal that Af12050 and TqaB represent a small subset of monomodular NRPSs with the A-T-C domain architecture. Future studies investigating enzymatic logic similar to that catalyzed by Af12050 and TqaB will be of value to more fully characterize the intriguing functionality of this subset of terminal C-domains. Additionally, as the number of known Af12050 and TqaB homologues increases, it is intriguing to postulate that it may be possible to provide a sequence-based prediction of the stereospecificity of C−N bond formation in analogous couplings of amino acids to oxidized indolic scaffolds.

A series of metabolites have been identified from a variety of fungal sources that appear to be derived from amino acid coupling similar to that catalyzed by Af12050 and TqaB (for representative examples, see Figure S11A of the Supporting Information). The population of analogous compounds with relative stereochemistry matching that of FQA (in which the relative orientation of the oxy-indole-derived hydroxyl to the C−N bond formed during the amino acid addition is *trans*) and those with relative stereochemistry matching that of 2′-*epi*-FQA (in which the relative orientation is *trans*) appears to be approximately equal. It is interesting to reason that bioinformatic analysis of the currently unidentified gene clusters responsible for the biosynthesis of chaetominine and asperlicin would reveal a monomodular NRPS with a terminal C-domain more similar to that of Af12050 than that of TqaB, whereas lumpidin and fiscalin biosynthetic gene clusters may reveal a monomodular NRPS with a terminal C-domain more similar to that of TqaB than that of Af12050 (Figure S11B of the Supporting Information).

In conclusion, herein we describe the utilization of homologous enzymes from two different biosynthetic pathways to illustrate the mediation of stereospecific C−N bond formation by the catalytic action of a terminal C-domain of fungal NRPSs. Investigations with full-length proteins, C-domain-swapped chimeric proteins, and the corresponding stand-alone C-domains with the required substrates all prove the C-domain is necessary and sufficient to control the stereochemistry around the observed five-member ring. The mechanism of control over the stereospecific addition remains unclear despite efforts to probe the order of steps involved.

Phylogenetic comparison of terminal C-domains observed in these types of systems illustrates a clear division from that of canonical C-domains involved in typical amide bond formation. This suggests a clear evolutionary pathway for C-domains of this type devised to increase the complexity of NRPS-synthesized peptides by carefully tailoring with moieties of strictly controlled stereochemistry.

■ ASSOCIATED CONTENT

Supporting Information. Figures providing sequence alignments of TqaH and Af12060 (Figure S1) and TqaB and Af12050 (Figure S2), comparison of loading of Af12050 and TqaB stand-alone T-domains (Figure S3), time courses of both spontaneous and enzymatic 2′-*epi*-FQA formation (Figure S4), depictions of protein purity illustrated by sodium dodecyl sulfate−polyacrylamide gel electrophoresis and estimation of flavin content of monooxygenases Af12060 and TqaH (Figure S5), UV absorbance spectra of FQ scaffold compounds (Figure S6), substrate specificities of chimera **1** and chimera **2** (Figures S7 and S8), synthesis of L-Ala SNAC and analogues (Figure S9), phylogenetic analysis of fungal monomodular A-T-C NRPSs (Figure S10), and additional examples of fungal metabolites with relative stereochemistries like those of FQA or 2′-*epi*-FQA (Figure S11) and tables showing primers used in this work (Table S1) and NMR spectroscopic characterization of FQF diol (Table S2) and 2′-*epi*-FQA (Table S3). This material is available free of charge via the Internet at http://pubs.acs.org.

■ AUTHOR INFORMATION

Corresponding Author

*E-mail: christopher_walsh@hms.harvard.edu. Phone: (617) 432-1715. Fax: (617) 432-0483.

Author Contributions

S.W.H. and B.D.A. contributed equally to this work.

Funding Sources

This work is supported in part by National Institutes of Health Grants GM20011 (to C.T.W.), F32GM090475 (postdoctoral fellowship to B.D.A.), and 1R01GM092217 (to Y.T.).

■ ACKNOWLEDGMENT

We thank Elizabeth Sattely for providing purified *B. subtilis* Sfp and Steven Malcolmson for helpful discussion.

■ ABBREVIATIONS

2-AIB, 2-aminoisobutyric acid; A, adenylation; AMP, adenosine 5′-monophosphate; Ant, anthranilate (2-aminobenzoate); BOC, *tert*-butyloxycarbonyl; BSA, bovine serum albumin; CoA, coenzyme A; CV, column volumes; DAD, diode-array detector; DCM, dichloromethane; DMSO, dimethyl sulfoxide; EDTA, ethylenediaminetetraacetic acid; *epi*, epimer; FAD, flavin adenine dinucleotide; FQA, fumiquinazoline A; FQC, fumiquinazoline C; FQD, fumiquinazoline D; FQF, fumiquinazoline F; *gem*, geminal; ESI, electrospray ionization; HPLC, high-performance liquid chromatography; HRMS, high-resolution mass spectra; IPTG, isopropyl β-D-galactopyranoside; LB, Luria-Bertani medium; LC−MS, liquid chromatography−mass spectrometry; LIC, ligation-independent cloning; MeCN, acetonitrile; NADH, nicotinamide adenine dinucleotide; Ni-NTA, nickel nitrilotriacetic acid-agarose; NMR, nuclear magnetic resonance; NRPS, nonribosomal

peptide synthetase; PCR, polymerase chain reaction; PPT, 4′-phosphopantetheine; PPtase, phosphopantetheinyl transferase; PyBOP, benzotriazol-1-yloxytripyrrolidinophosphonium hexafluorophosphate; QTOF, quadrupole time-of-flight; RT-PCR, reverse transcription polymerase chain reaction; SNAC, *N*-acetylcysteamine thioester; SPE, solid phase extraction; TCA, trichloroacetic acid; TFA, trifluoroacetic acid; THF, tetrahydrofuran; TQA, tryptoquialanine; Tris, tris(hydroxymethyl)aminomethane.

REFERENCES

(1) Daniel, J. F. d. S., and Rodrigues Filho, E. (2007) Peptaibols of *Trichoderma*. *Nat. Prod. Rep. 24*, 1128–1141.

(2) Pruksakorn, P. et al. (2010) et al. Trichoderins, novel aminolipopeptides from a marine sponge-derived *Trichoderma* sp., are active against dormant mycobacteria. *Bioorg. Med. Chem. Lett. 20*, 3658–3663.

(3) Peltola, J. et al. (2004) et al. Biological effects of *Trichoderma harzianum* peptaibols on mammalian cells. *Appl. Environ. Microbiol. 70*, 4996–5004.

(4) DeBattista, C. (2009) Antidepressant agents. In *Basic & Clinical Pharmacology* (Katzung, B. G., Ed.) 11th ed., McGraw-Hill, New York.

(5) Meltzer, H. (2009) Antipsychotic agents & lithium. In *Basic & Clinical Pharmacology* (Katzung, B. G., Ed.) 11th ed., McGraw-Hill, New York.

(6) Zhao, S. et al. (2002) et al. Biological activity of the tryprostatins and their diastereomers on human carcinoma cell lines. *J. Med. Chem. 45*, 1559–1562.

(7) Rabindran, S. K. et al. (2000) et al. Fumitremorgin C reverses multidrug resistance in cells transfected with the breast cancer resistance protein. *Cancer Res. 60*, 47–50.

(8) Cole, R. J. (1981) Fungal tremorgens. *J. Food Prot. 44*, 715–722.

(9) Valdes, J. J. et al. (1985) et al. Aflatrem: A tremorgenic mycotoxin with acute neurotoxic effects. *Environ. Health Perspect. 62*, 459–463.

(10) Gao, X. et al. (2011) et al. Fungal indole alkaloid biosynthesis: Genetic and biochemical investigation of the tryptoquialanine pathway in *Penicillium aethiopicum*. *J. Am. Chem. Soc. 133*, 2729–2741.

(11) Numata, A. et al. (1992) et al. Fumiquinazolines, novel metabolites of a fungus isolated from a saltfish. *Tetrahedron Lett. 33*, 1621–1624.

(12) Frisvad, J. C. et al. (2009) et al. Metabolomics of *Aspergillus fumigatus*. *Med. Mycol. 47*, S53–S71.

(13) Finking, R., and Marahiel, M. A. (2004) Biosynthesis of nonribosomal peptides. *Annu. Rev. Microbiol. 58*, 453–488.

(14) Schwarzer, D. et al. (2003) et al. Nonribosomal peptides: From genes to products. *Nat. Prod. Rep. 20*, 275–287.

(15) Strieker, M. et al. (2010) et al. Nonribosomal peptide synthetases: Structures and dynamics. *Curr. Opin. Struct. Biol. 20*, 234–240.

(16) Eisfeld, K. (2009) Non-ribosomal peptide synthetases of fungi. In *Physiology and Genetics: Selected Basic and Applied Aspects* (Anke, T., and Weber, D., Eds.) Springer-Verlag, Heidelberg, Germany.

(17) Cramer, R. A., Jr. et al. (2006) et al. Phylogenomic analysis of non-ribosomal peptide synthetases in the genus *Aspergillus*. *Gene 383*, 24–32.

(18) Maiya, S. et al. (2006) et al. The fumitremorgin gene cluster of *Aspergillus fumigatus*: Identification of a gene encoding brevianamide F synthetase. *ChemBioChem 7*, 1062–1069.

(19) Weber, G. et al. (1994) et al. The peptide synthetase catalyzing cyclosporine production in *Tolypocladium niveum* is encoded by a giant 45.8-kilobase open reading frame. *Curr. Genet. 26*, 120–125.

(20) Sussmuth, R. et al. (2011) et al. Fungal cyclooligomer depsipeptides: From classical biochemistry to combinatorial biosynthesis. *Nat. Prod. Rep. 28*, 99–124.

(21) Eisendle, M. et al. (2003) et al. The siderophore system is essential for viability of *Aspergillus nidulans*: Functional analysis of two genes encoding L-ornithine N5-monooxygenase (sidA) and a nonribosomal peptide synthetase (sidC). *Mol. Microbiol. 49*, 359–375.

(22) Gao, X., and Tang, Y. (2011) personal communication.

(23) Ames, B. D. et al. (2010) et al. Enzymatic processing of fumiquinazoline F: A tandem oxidative-acylation strategy for the generation of multicyclic scaffolds in fungal indole alkaloid biosynthesis. *Biochemistry 49*, 8564–8576.

(24) Wilkins, M. R. et al. (1999) et al. Protein identification and analysis tools in the ExPASy server. *Methods Mol. Biol. 112*, 531–552.

(25) Soding, J. et al. (2005) et al. The HHpred interactive server for protein homology detection and structure prediction. *Nucleic Acids Res. 33*, 244–248.

(26) Pfeifer, B. A. et al. (2001) et al. Biosynthesis of complex polyketides in a metabolically engineered strain of *E. coli*. *Science 291*, 1790–1792.

(27) Quadri, L. E. et al. (1998) et al. Characterization of Sfp, a *Bacillus subtilis* phosphopantetheinyl transferase for peptidyl carrier protein domains in peptide synthetases. *Biochemistry 37*, 1585–1595.

(28) Samel, S. A. et al. (2007) et al. Structural and functional insights into a peptide bond-forming bidomain from a nonribosomal peptide synthetase. *Structure 15*, 781–792.

(29) Ames, B. D., et al. (2010) unpublished observations.

(30) Roche, E. D., and Walsh, C. T. (2003) Dissection of the EntF condensation domain boundary and active site residues in nonribosomal peptide synthesis. *Biochemistry 42*, 1334–1344.

(31) Stachelhaus, T. et al. (1995) et al. Rational design of peptide antibiotics by targeted replacement of bacterial and fungal domains. *Science 269*, 69–72.

(32) Fischbach, M. A. et al. (2007) et al. Directed evolution can rapidly improve the activity of chimeric assembly-line enzymes. *Proc. Natl. Acad. Sci. U.S.A. 104*, 11951–11956.

(33) Mootz, H. D. et al. (2000) et al. Construction of hybrid peptide synthetases by module and domain fusions. *Proc. Natl. Acad. Sci. U.S.A. 97*, 5848–5853.

(34) Ehmann, D. E. et al. (2000) et al. Aminoacyl-SNACs as small-molecule substrates for the condensation domains of nonribosomal peptide synthetases. *Chem. Biol. 7*, 765–772.

(35) Sattely, E. S., and Walsh, C. T. (2008) A latent oxazoline electrophile for N−O−C bond formation in pseudomonine biosynthesis. *J. Am. Chem. Soc. 130*, 12282–12284.

(36) Keating, T. A. et al. (2000) et al. Vibriobactin biosynthesis in *Vibrio cholerae*: VibH is an amide synthase homologous to nonribosomal peptide synthetase condensation domains. *Biochemistry 39*, 15513–15521.

(37) Ehmann, D. E. et al. (1999) et al. Lysine biosynthesis in *Saccharomyces cerevisiae*: Mechanism of α-aminoadipate reductase (Lys2) involves posttranslational phosphopantetheinylation by Lys5. *Biochemistry 38*, 6171–6177.

(38) Torruella, G. et al. (2009) et al. The evolutionary history of lysine biosynthesis pathways within eukaryotes. *J. Mol. Evol. 69*, 240–248.

(39) Ames, B. D., and Walsh, C. T. (2010) Anthranilate-activating modules from fungal nonribosomal peptide assembly lines. *Biochemistry 49*, 3351–3365.

(40) Rausch, C. et al. (2007) et al. Phylogenetic analysis of condensation domains in NRPS sheds light on their functional evolution. *BMC Evol. Biol. 7*, 78.

(41) Larkin, M. A. et al. (2007) et al. Clustal W and Clustal X version 2.0. *Bioinformatics 23*, 2947–2948.

(42) Bushley, K., and Turgeon, B. G. (2010) Phylogenomics reveals subfamilies of fungal nonribosomal peptide synthetases and their evolutionary relationships. *BMC Evol. Biol. 10*, 26.